Seasonal changes in the photophysiology of Ulva batuffolosa in a coastal barrier reef

Thierry Jauffrais, Maele Brisset, Laura Lagourgue, Claude Payri, Siloë Gobin, Romain Le Gendre, Simon van Wynsberge

▶ **To cite this version:**

Thierry Jauffrais, Maele Brisset, Laura Lagourgue, Claude Payri, Siloë Gobin, et al.. Seasonal changes in the photophysiology of Ulva batuffolosa in a coastal barrier reef. Aquatic Botany, 2022, 179, 103515 (9p.). 10.1016/j.aquabot.2022.103515 . hal-04203755

HAL Id: hal-04203755
https://hal.science/hal-04203755

Submitted on 22 Jul 2024

HAL is a multi-disciplinary open access archive for the deposit and dissemination of scientific research documents, whether they are published or not. The documents may come from teaching and research institutions in France or abroad, or from public or private research centers.

L'archive ouverte pluridisciplinaire **HAL**, est destinée au dépôt et à la diffusion de documents scientifiques de niveau recherche, publiés ou non, émanant des établissements d'enseignement et de recherche français ou étrangers, des laboratoires publics ou privés.

Distributed under a Creative Commons Attribution - NonCommercial 4.0 International License

Version of Record: https://www.sciencedirect.com/science/article/pii/S0304377022000274
Manuscript_58b0b501ad3e314163843d47bf19c01d

Seasonal changes in the photophysiology of *Ulva batuffolosa* in a coastal barrier reef

Thierry Jauffrais[1*], Maële Brisset[1], Laura Lagourgue[2], Claude E. Payri[2], Siloë Gobin[2], Romain Le Gendre[1], Simon Van Wynsberge[1]

[1] Ifremer, IRD, Univ Nouvelle-Calédonie, Univ La Réunion, CNRS, UMR 9220 ENTROPIE, BP 32078, 98800, Nouméa, New Caledonia

[2] IRD, Ifremer, Univ Nouvelle-Calédonie, Univ La Réunion, CNRS, UMR 9220 ENTROPIE, BP A5, 98848 Nouméa cedex, New Caledonia

*Corresponding authors:

thierry.jauffrais@ifremer.fr; Tel.: +687-352-571; Orcid: 0000-0001-9681-6239

Abstract:

To assess the photophysiological capacity of the recently described *Ulva batuffolosa* to form blooms in coral reefs, we monitored its biomass and photophysiological capacity with pulse amplitude modulated (PAM) fluorometry over a year period on a coastal barrier reef in New Caledonia, along with temperature and light. Effective and maximum quantum efficiencies of the photosystem II measured on this *Ulva* species indicated that the algae was in a "good health" all over the year with high quantum efficiencies under either light (Fq'/Fm') or dark incubated conditions and (Fv/Fm). Photo-acclimation and -regulation status used by this *Ulva* sp. were driven by seasons (*i.e.*, light and temperature) in the lagoon. Although photo-inhibition was an evidence during the warm period, *U. batuffolosa* was overall well adapted to tolerate the range of irradiance and temperature that characterized the lagoon over the year, which suggests that photosynthesis is not an impediment to green tides by this species.

Key words: bloom, coral reef, chlorophyte, pulse amplitude modulated fluorometer, *Ulva batuffolosa*, rapid light curve, NPQ

© 2022 published by Elsevier. This manuscript is made available under the CC BY NC user license
https://creativecommons.org/licenses/by-nc/4.0/

Highlights :

- Photo-acclimation and regulation status of *Ulva batuffolosa* were modulated by season
- *Ulva batuffolosa* was well adapted to support and tolerate high irradiance
- The combination of elevated temperatures and light damaged its physiology

1. Introduction

The photophysiological capacity of *Ulva* species is a key factor that determine their ability to form massive blooms (Cui et al., 2015; Wang et al., 2016; Huo et al., 2021), but it has mainly been characterized in temperate areas and subtropical estuaries, e.g., the Yellow sea, the southern coast of Brazil and Florida (Scherner et al., 2012; Xu et al., 2014; Whitehouse and Lapointe, 2015; Zhang et al., 2015, Huo et al., 2021). By contrast, the photophysiological response of *Ulva* species to face environmental stresses is not clearly defined in tropical and subtropical shallow coral reef lagoons. In these lagoons, temperature is higher than in temperate ecosystems, and light can be higher over longer period. These habitats are characterized by clear waters with a high penetration depth of the photosynthetically active radiation (PAR), up to 2000 µmol m^{-2} s^{-1} (Kirk, 1994; Pringault et al., 2005), and ultraviolet radiation, up to 2 W m^{-2} for UVB and 40 W m^{-2} for UVA (Torregiani and Lesser, 2007; Conan et al., 2008; Courtial et al., 2017). In fact, light intensity may fluctuate significantly from second to seasonal scale, with fluctuations that are predictable (e.g., day length and light angle, tide) and others that are not (e.g., cloudiness, lagoon turbidity caused by terrestrial run-off or sediment resuspension). In these habitats, *Ulva* must cope with fluctuating light to optimize its use for photosynthesis and to protect their photosystems from excessive light (Henley and Ramus, 1989; Carr and Björk, 2007, Goss and Jakob, 2010; Zhang et al., 2015). Previous studies on temperate species highlighted the great ability and plasticity of *Ulva* to cope with light (Carr and Björk, 2007, Zhang et al., 2015). *Ulva* species (e.g., *U. prolifera* and *U. lactuca*) were able to keep high photosynthetic capability using the plasticity of the surface and lower layers of their thalli, modifying their pigment content and using NPQ, D1 protein, energy redistribution between PSII/PSI and fast recovery ability under low light to avoid irreversible damage to their PSII and PSI (Carr and Björk, 2007; Zhang et al., 2015; Wang et al., 2016).

Algae exposed to excessive light energy can implement three processes: photo-adaptation, acclimation and regulation (Falkowski and Laroche, 1991; Raven and Geider, 2003; Huot and Babin, 2010). Photo-adaptation is a long term and genetic process, while photo-acclimation is explained by the macromolecular modification of a species from hours to days/seasonal light conditions (Falkowski and Laroche, 1991; Raven and Geider, 2003; Huot and Babin, 2010). At this time scale, the genetic make-

up does not change but the algae can modify the number and size of its photosynthetic apparatus and associated pigments. Finally, photo-regulation processes are more dedicated to manage rapid changes in the light regimes (seconds to minutes) to quickly protect (lower or prevent damages) photosystems from excessive light energy, but without *de novo* synthesis or break down of molecules (Falkowski and Laroche, 1991; Raven and Geider, 2003; Huot and Babin, 2010). It can be achieved by quenching the photochemistry through non-photochemical processes, which dissipates the excitations in the antennae complex into heat (Consalvey et al., 2005).

Photosynthesis irradiance curves have been used in the past to assess the effect of environmental factors on macroalgae physiology (Lapointe, 1981), including *Ulva* species (Figueroa et al., 2009; Scherner et al., 2012; Xu et al., 2014; Whitehouse and Lapointe, 2015; Wang et al., 2016). In this scenario, pulse amplitude modulated (PAM) fluorometry is a powerful and commonly used technique based on chlorophyll *a* fluorescence (Krause and Weis, 1991; Schreiber et al., 1994; Maxwell and Johnson, 2000). It offers the advantage to be fast (Schreiber et al., 1994) and is often used to assess photophysiological response of micro and macroalgae under stressful conditions (Figueroa et al., 1997; Figueroa et al., 2009; Scherner et al., 2012; Whitehouse and Lapointe, 2015; Coulombier et al., 2021). Although it has proven to be a useful and powerful tool for the studies of macroalgae photophysiology (Ralph and Gademann, 2005), this approach is often considered biased for macroalgae. Variations in the fluorescence signal due to the thickness of macroalgae tissues often hampers direct comparison with oxygenic photosynthesis measurements particularly at high irradiance and comparison between species (reviewed in Enriquez and Borovitzka, 2010). Although imperfect, the use of relative electron transport rate (rETR) values instead of ETR is recommended to reduce problems associated with absorptance (*i.e.*, the fraction of incident light absorbed by pigmented tissue) particularly if the organisms or tissues examined have similar absorption cross-sections (Beer et al. 2001; Ralph et al., 2002; Enriquez and Borovitzka, 2010). PAM fluorometry also allows to characterize photophysiological state, through the study of dark and light incubated algae. Light incubated algae have their photosynthetic apparatus adapted to manage the ambient light, *i.e.*, all photo-regulation processes are active; whereas, dark incubated algae have downregulated all

89 photosynthetic mechanisms that usually help the algae to cope with the ambient light but without
90 modifying their acclimated macromolecular compounds (Huot and Babin, 2010).
91 In this study, we monitored the photophysiological capacity of *Ulva batuffolosa*, a species involved in
92 green tides, in a shallow tropical lagoon in New Caledonia, over a year period. We collected the *Ulva*
93 *sp.* at different seasons and used PAM fluorometry to quantify their PSII quantum efficiency,
94 maximum relative electron transport rate, their capacity to cope with light at low and high irradiance
95 under light or dark incubated conditions, and to dissipate the excess of energy via Non-Photochemical
96 Quenching (NPQ). All measurements were acquired to provide an overview of the physiological state
97 of *Ulva batuffolosa* owing to environmental and seasonal (light and temperature) photo-acclimation
98 and photo-regulation status.
99
100 **2. Materials and method**
101 *2.1. Study area*
102 New Caledonia is located in the Southwestern Pacific Ocean, ~1 500 km east of Australia (Fig. 1). It
103 comprises one main large island, known as Grande Terre, bordered by a 1 600 km long barrier reef,
104 which delimits a 23 400 km² lagoon (Andréfouët et al., 2009). The present study focuses on the Poé-
105 Gouaro-Déva (PGD) lagoon (21.62°S, 165.38°E) located on the west coast of Grande Terre (Fig. 1), a
106 hotspot of tourism activities and one of the Caledonian lagoons registered at the UNESCO World
107 Heritage sites. In this study, we focus on green algal mats located around B21 station in the
108 northwestern part of the PGD lagoon (Fig. 1), at the limit between a wide seagrass bed that borders the
109 coastline and sandy soft-bottom habitats. Blooms of *U. batuffolosa* in this area were the main cause of
110 the two green tides that occurred in January 2018 and June 2019 (Brisset et al., 2021; Lagourgue et al.,
111 *in press*). In this shallow area (maximum depth ~2 m), the seagrass bed is not homogeneous and can
112 be intertwined with patches of coral communities (branching *Montipora* and *Acropora*) and sand.
113
114 *2.2. Field sampling*
115 Five field campaigns were performed at 2-4 months intervals to collect green algae and estimate their
116 cover, the 16th May 2019, 09th July 2019, 18th November 2019, 19th February 2020, and 25th May

2020, respectively. The cover of green macroalgae was estimated along three line intersect transects of 10 m length. Transects were not permanently established, but their location was geo-referenced (handheld GPS Garmin) with a 10–20 m uncertainty, and they were always performed at similar depth and on the same habitat. Along each transect, two to three 0.25 m² quadrats were placed on algal patches. All green algae inside quadrats were collected and stored in plastic bags in a cooler for further analyses. For the three last field campaigns, as *Ulva* were rare and absent on transects (see results), samples were collected within a larger screening area (~ 10 000 m²) around transects.

2.3 Temperature and light condition before and during sampling

Light and temperature that affected the area all along the study period were acquired using regional models and *in situ* instruments.

Light above the water surface was measured during each field campaign using a light meter (Li-cor) and a Li-192 quantum sensor (Li-cor). Light conditions that characterized the PGD area before and during sampling were also extracted from the ERA5 atmospheric reanalysis (Hersbach et al., 2020). This model provides an hourly time series of variables such as the Surface Solar Radiation Downwards (SSRD, KJ m^{-2}) with a one hour time step at 0.25° long and 0.25° lat spatial resolution. For this study, we used data extracted from the nearest grid point to the PGD lagoon (21.75°S 165.25°E).

Lagoon temperature was recorded from February 2019 to May 2020 at station B21, or near to it, with high accuracy (±0.002 °C) using RBR® duo loggers. Since gaps affected the time series during one inter-season (no data recorded between 16th May and 09th July 2019), the time series was filled with satellite derived sea surface temperature (SST) estimates. Sea surface temperature was extracted from the Global, daily Multi-scale Ultra-high Resolution (MUR) SST analysis at 0.01° (around 1 km) resolution (Chin et al., 2017; https://mur.jpl.nasa.gov/). Data were also retrieved from the nearest grid point from field transects. Comparison with *in situ* temperature data recorded by the logger and SST estimates highlighted a median difference of ± 0.7 °C. The maximum daily difference reached 2.7 °C during the warm period, but SST data were deemed suitable for the purpose of this study since lower bias were found during inter-seasons (Supplement material SM1).

145

146 *2.4. Algae biomass estimation*

147 The biomass of green algae collected inside each quadrat was determined, all genera confounded.
148 Algae were weighted after sampling (wet weight), and after a drying period at 50°C until a constant
149 weight value was obtained. The resulting biomass (dry weight) was averaged among quadrats (B_Q, g
150 m^{-2}) and pondered by the percentage of cover of green algae along the transect (C_T, %) to infer
151 biomass at transect scale (B_T, g m^{-2}, equation 1).

152 $$B_T = B_Q \times C_T \quad \text{(eq. 1)}$$

153

154 *2.5. Algae identification*

155 The specimens sampled along each transect were sorted under binocular, pressed-dried on herbarium
156 sheets and housed at NOU (herbarium abbreviation follows Thiers (2019)). Fragments were
157 subsampled and preserved in a formaldehyde solution (5% in seawater added with borax) for further
158 taxonomical analysis and ethanol 95% for DNA analyses. Morphological and histological observations
159 were performed using an Axio Imager A2 microscope (ZEISS, Oberkochen, Germany) fitted with a
160 Canon EOS 100D camera (Canon, Tokyo, Japan). Species identification were based on the most
161 relevant literature references for *Ulva* species, including Kraft et al. (2010), Horimoto et al. (2011),
162 Masakiyo et al. (2014), Krupnik et al. (2018), Melton et al. (2020) and Xie et al. (2020). DNA
163 analyses were conducted separately and are part of a comprehensive phylogenetic and molecular
164 taxonomy study of the Ulvales from New Caledonia (Lagourgue et al. *in press*).

165

166 *2.6. Photosynthetic parameters of* Ulva batuffolosa *over a one-year-period*

167 Pulse Amplitude Modulated (PAM) fluorometry measurements were performed during each field
168 campaigns, to provide an overview of the physiological state of the bloom forming *U. batuffolosa* in a
169 diversity of environmental conditions. All measurements were performed under light or dark incubated
170 conditions to discriminate photo-acclimation and photo-regulation status.

171 Photosynthetic parameters were measured with a PAM chlorophyll fluorometer (AquaPen-P AP 110-P
172 of Photon Systems Instruments, Czech Republic) with a blue light at 470 nm. All measurements were
173 carried in a Petri dish (10 cm × 1.5 cm) filled with filtered sea water (50-75 mL, 0.2 µm) on the apical
174 region of *U. batuffolosa* to avoid a potential impact of self-shaded region. Following microscopic
175 identification, fragments of apical regions were cut and maintained with a perpendicular orientation
176 under the submersible optical probe of the PAM fluorometer. The set up was then placed in a black box
177 to avoid disturbance of ambient light during measurements. All measurements were done in triplicate,
178 each time on new fragments to avoid trouble due to light exposure from previous measurements.
179 Light incubated measurements were carried out immediately after sampling on the boat (Aldric, 5.6 m
180 Stabicraft), while, dark measurements were carried out following a dark (very low light 1-
181 2 µmol photons m^{-2} s^{-1}) adaptation of one hour in the laboratory. In between, the samples were kept in
182 relative darkness (2 µmol photons m^{-2} s^{-1}) in a cooler during transport to the laboratory, with a small
183 amount of *Ulva* in a large quantity of seawater (2 L) from the sampling site.
184 The effective and maximum PSII quantum efficiency (Fq'/Fm' and Fv/Fm) were measured under light
185 and dark incubated conditions, respectively. These measures were acquired with a saturating pulse at
186 3000 µmol photons m^{-2} s^{-1} (Table 1; Schreiber et al., 1994; Consalvey et al., 2005).
187 Rapid light curves were performed under light and dark incubated conditions with seven incremental
188 irradiances steps (10; 20; 50; 100; 300; 500 and 1 000 µmol photons m^{-2} s^{-1}) of 60 s. The *Ulva*
189 photophysiological parameters ($rETR_{max}$ (AU), alpha (α), beta (β) and Ek) were estimated by adjusting
190 the model by Platt et al. (1980) to the experimental data (Table 1). In addition, the photo regulation
191 capacity via Non-Photochemical Quenching (NPQ) was measured to assess the photo-regulation
192 capacity and recovery of the *Ulva* sp. reaction centers to a continuous illumination of
193 1 000 µmol photons m^{-2} s^{-1} with 10 successive light pulses at saturating light and followed by darkness
194 for recovery with two quantum efficiency measurements (only on dark incubated *Ulva*). These NPQ
195 measurements; however, could not be performed during the first field campaign because of a technical
196 problem (Table 1).
197
198 *2.7. Statistical analyses*

To test statistically the differences in environmental history conditions that affected green algae collected between field campaigns, we used the conditions of light (SSRD) and temperature that occurred along the week before sampling each campaign. Statistical differences between campaigns were tested using ANOVA or Kruskal–Wallis tests when the homoscedasticity and normality hypotheses were not satisfied. When necessary, Fisher's least significant difference (LSD) tests were performed after ANOVA and Dunn's tests were performed after Kruskal-Wallis tests to assess the significance of differences between each pair of sampling campaigns. Correlation between photo-physiological parameters ($rETR_{max}$, alpha, beta, Ek) and environmental parameters (temperature, SSRD, PAR) were tested using the Spearman's non-parametric correlation test. For NPQ, a generalized linear model was used to assess differences between sampling campaigns, and time points generated by repeated NPQ measurements during the NPQ induction by actinic light and dark recovery period. The statistical analyses were carried out using the R studio v1.2.1578 software (©2009–2019 R studio v1.2.1578) for the environmental data and Statgraphics Centurion XV.I (StatPoint Technologies) for the photophysiological data. All results (*i.e.*, PAM measurements and environmental characterization) are expressed as mean ± standard error (SE) in this manuscript.

3. Results

3.1. Temperature and light conditions experienced by collected algae

Over the study period, seawater temperature ranged from 21.46 °C in August 2019 to 29.59 °C in March 2020, with significant short-term variation (Fig. 2). This include a decrease of 2.83 °C in 5 days the week before sampling in July 2019, and an increase of 3.75 °C in 13 days at the end of November 2019. As a result, the *Ulva* species collected during the field campaigns were exposed to different history of temperatures (KW Chi-squared = 29.54; $p < 0.001$), with significantly higher temperature measured in February 2020 (28.09 ± 0.89 °C) before sampling than before all other campaigns (Dunn's test Z ranging between -4.30 and 4.64; $p < 0.05$), except for the May 2019 campaign ($Z = 1.82$; $p = 0.06$; Supplement material SM2). In July 2019 and May 2020, the algae were exposed to periods of lower temperatures, *i.e.*, 23.27 ± 1.31 °C and 24.13 ± 0.44 °C, respectively. The

226 temperature history experienced by algae sampled in May 2019 and November 2020 were similar
227 (25.53 ± 0.25 °C and 25.40 ± 0.77 °C, p = 0.86, Fig. 2).
228 Surface Solar Radiation Downwards (SSRD) also followed a seasonal pattern, but reached highest
229 values in late November 2019 (longest days) and lower values in early June (shortest days, Fig. 2). As
230 a result, the *Ulva* collected during the different field campaigns were exposed to different light history
231 (KW Chi-squared = 23.52; $p < 0.001$), with higher values in November 2019 (2 111 ± 1 345 KJ m^{-2})
232 than during the other sampling periods (Dunn's test Z ranging from -3.28 to 4.40, $p < 0.01$). The
233 lowest SSRD were measured the weeks before July 2019 (893 ± 787 KJ m^{-2}), May 2019
234 (991 ± 868 KJ m^{-2}), and May 2020 (1 065 ± 884 KJ m^{-2}) field campaigns. Photosynthetic Active
235 Radiation (PAR) measured during field campaigns were higher in November 2019
236 (2042 ± 51 µmol photons m^{-2} s^{-1}), than during other field campaigns (May 2019,
237 1746 ± 41 µmol photons m^{-2} s^{-1}; July 2019, 1838 ± 43 µmol photons m^{-2} s^{-1}; February 2020,
238 1921 ± 42 µmol photons m^{-2} s^{-1}). The lowest values of PAR were found in May 2020,
239 344 ± 36 µmol photons m^{-2} s^{-1}), because of a cloudy weather during this last field campaign.
240
241 *3.2. Biomass of green algae*
242 Green algae were abundant during the first two field campaigns, with higher biomass in July 2019
243 (B_T = 69.83 ± 17.10 gDW m^{-2}) than in May 2019 (B_T = 8.80 ± 1.59 gDW m^{-2}). During the three other
244 field campaigns, green algae were rare, with no biomass along the three transects nor inside quadrats
245 (Fig. 3). However, *Ulva batuffolosa* was still present around transects.
246
247 *3.3. Algae identification*
248 Among the macroalgae identified along or nearby transects in this study, *Ulva batuffolosa* was largely
249 predominant. This species forms dense and moving tufts of entangled, tubular, and branched
250 filaments. Main axes are variable in size but usually measure ~100 µm or more in diameter, while
251 secondary branches are smaller. They are composed of rectangular to polygonal cells (20*25*20 µm)
252 with regular contours, forming a coherent mat (Lagourgue et al. *in press*; Supplement Material SM3)

253 of several decimeters in length. They can attach to corals and seagrass, or drift in the water with the
254 currents. This species corresponds to *Ulva* sp.3 in Brisset et al. (2021).
255
256 *3.4. Photosynthetic parameters of the* Ulva *sp.*
257 The effective (Fq'/Fm') and maximum quantum (Fv/Fm) light utilization efficiency of the *Ulva* sp.,
258 *i.e.*, a proxy of the efficiency of the PSII in using light for photochemical conversion, measured under
259 light and dark incubated condition showed high values with Fq'/Fm' = 0.45 ± 0.6 and
260 Fv/Fm = 0.66 ± 0.05, but did not show very high differences between the five studied periods. No
261 significant differences between campaigns were found for Fq'/Fm' ($p = 0.10$) and solely the Fv/Fm
262 measured during the last sampling period in May 2020 was significantly lower ($p = 0.042$, Fv/Fm =
263 0.58 ± 0.03) than the other ones (Fv/Fm > 0.66, Fig 4B, Table 2).
264 Differences between sampling campaigns were clearly visible using the data extracted from the RLCs
265 (Table 2, Fig 5 and 6). The maximum electron transport rate ($rETR_{max}$) measured under light or dark
266 incubated conditions were both significantly different with P values below 0.01 (Table 2). This proxy
267 of the photosynthetic activity increased from May 2019 (70 ± 5 AU light incubated condition, 119 ± 2
268 AU dark incubated condition) to July 2019 (105 ± 4 AU light incubated condition and 131 ± 2 AU
269 dark incubated condition) and then decreased. Light incubated $rETR_{max}$ values were not statistically
270 different from November 2019 until the end of the survey (Fig. 6A, yellow bars); whereas the decrease
271 was more gradual regarding dark incubated values (Fig. 6A, grey bars).
272 Similarly, the light saturation coefficient (Ek), used here as a proxy of *U. batuffolosa* ability to use
273 "high light" intensity, was also significantly higher in July 2019 than for other sampling campaigns,
274 either for light incubated measurements (534 ± 43 µmol photons m^{-2} s^{-1} versus between 140 and
275 240 µmol photons m^{-2} s^{-1}, $p < 0.001$) and for dark incubated measurements (526 ± 23 µmol photons m^{-2} s^{-1} *versus* between 300 and 380 µmol photons m^{-2} s^{-1}, $p < 0.05$, Fig 6B and Table 2).
277 The maximum light utilization coefficients, alpha (α), used as a proxy of the algal ability to use "low
278 light" intensity, were also significantly different between periods (Fig 6C and Table 2), but these
279 differences were weaker compared to $rETR_{max}$ and E_k (Table 2). The lowest alpha values were
280 observed in July 2019 (0.21 ± 0.01 light incubated condition and 0.25 ± 0.02 dark incubated condition)

and the highest one in May 2019 (0.31 ± 0.04 light incubated condition and 0.32 ± 0.01 dark incubated condition).

The photoinhibition coefficient, beta (β) (Fig 6D; Table 2), was significantly different from zero for RLCs carried out under light incubated condition in February and May 2020 only (Fig 5A), and was higher in February than in May 2020 ($p < 0.05$, Table 2).

The NPQ measurements induced by the actinic light (yellow background on Fig. 7) and dark recovery (grey background) period were implemented to assess the photo-regulation capacity (*i.e.*, the capacity to dissipate the excess of energy as heat) and recovery via NPQ during and following an exposure to light. During the four field campaigns for which NPQ measurements were performed (Fig. 7), July 2019 to May 2020, NPQ was used by the *Ulva* sp. to protect their PS against an excess of light energy. However, the magnitude of NPQ induction and recovery was significantly greater in February 2020 and lower in November 2019 (Fig. 7; Table 3). In addition, no NPQ recovery was observed in May 2020. No significant correlation between photo-physiological parameters and environmental data could be evidenced with the Spearman non-parametric correlation tests, but the correlation between beta (light incubated) and temperature was near the significant level (rho = 0,87; p = 0,054; Supplement Material SM4).

4. Discussion

The photosynthetic seasonal acclimation of *U. batuffolosa* was observable by comparing field campaigns using both light and dark incubated data. *U. batuffolosa* increased its light-harvesting capacity (high $rETR_{max}$) under "low-light" austral autumn/winter conditions (*i.e.*, May and July 2019, Fig. 5 and 6A). On the contrary, *U. batuffolosa* lowered its $rETR_{max}$ under "high-light" austral summer conditions (*i.e.*, November 2019 and February 2020, Fig. 5). Such acclimation can either be achieved by increasing the number or the size of photosynthetic units (Richardson et al., 1983; Falkowski and Laroche, 1991; Beer et al., 2014). When the number of photosynthetic units (PSU) increases (under low light condition) then both the antenna size and the number of reaction centers increase, enhancing the functionality of the photosynthetic apparatus (*i.e.*, higher rETRmax, alpha and Ek, Beer et al., 2014). Whereas, if only the size of photosynthetic units increases under low-light conditions, this should decrease the maximal photosynthetic productivity while increasing the light utilization

efficiency (alpha) (Richardson et al., 1983; Beer et al., 2014). In the present study, *U. batuffolosa* $rETR_{max}$ and E_k were higher for the *Ulva* collected during field campaigns characterized by lower irradiance (PAR) and SSRD history, while the response of alpha is unclear, indicating that photo-acclimation was achieved through the adjustment of the number of PSU to maximize light utilization during the lower light austral winter period rather than through the size of the PSU. However, algae collected in May 2020 escaped the trend, suggesting that acclimation capacity of algae was also dependent on other environmental factors (e.g., nutrient availability). N-limitation may gradually cause a decrease in photosynthetic pigments (Geider et al., 1993), a decline in Fv/Fm (Cleveland and Perry, 1987; Berges et al., 1996; Jauffrais et al., 2016) and the gradual inactivation of the protein D1 in PSII reaction centers (Campbell and Tyystjarvi, 2012). Protein D1 is a key component in the electron transport chain and its turnover is often a limiting factor in PSII repair rates (Campbell and Tyystjarvi, 2012).

In February 2020, *U. batuffolosa* was stressed by the environmental conditions, as shown by the presence of photoinhibition (beta > 0). Photoinhibition could be induced by the high light availability and the higher temperature (>28°C). In May 2020, although Fv/Fm was still relatively high, other photophysiological data indicated that *U. batuffolosa* was living under stressful conditions at the end of the study (rETRmax and β), which was supported by the decline and almost absence of *U. batuffolosa* biomass in the lagoon (Fig. 3). This decrease in photosynthetic capacity of *U. batuffolosa* over the study period probably result from the combined effect of season (light and temperature) and a suggested N-limitation, which could explain the decrease in $rETR_{max}$, finally leading to the induction of photoinhibition in February and May 2020.

Non-photochemical quenching (NPQ) is a common and important mechanism utilized by algae to tolerate and prevent damages to photosystems, owing to sudden high or fluctuating light levels, by heat dissipation of excessive light energy (Franklin et al., 1992;Uhrmacher et al., 1995; Schofield et al., 1998; Bischof et al., 2006; Enríquez and Borowitzka, 2010). *U. batuffolosa* utilized NPQ over all surveys, *i.e.*, during both austral summer and winter, owing to the high solar irradiance in New Caledonia all year around. NPQ is thus an important photo-regulation mechanism utilized by *U. batuffolosa* in the PGD lagoon, which allows to prevent or minimize photoinhibition in response to

short-term changes in irradiance and to maximize photosynthesis and productivity under the high irradiance of this shallow coral reef habitat.

However, NPQ can become exhausted under excessive light especially if amplified by other environmental pressure. Reduced NPQ efficiency and lower recovery capacity, such as the difference observed between February and May 2020, can damage protein D1 leading to a decline in photosynthetic efficiency, chronic photoinhibition and production of ROS (Franklin and Forster, 1997), which may be enhanced by high temperature and nutrient limitation (Franklin, 1994; Campbell et al., 2006). The decline of $rETR_{max}$ until the end of the study is thus probably due to the exhaustion of photo-regulation mechanisms (e.g., NPQ) leading to long-term photoinhibition triggered by the combination of high light and temperature.

5. Conclusion

This study highlights that photo-acclimation and -regulation status of *U. batuffolosa* are mainly driven by seasons (*i.e.*, light and temperature) in New Caledonia. In addition, our data provide significant advances in understanding the ability of this bloom forming species to use and manage light in clear and shallow water habitats. Notably, our study suggests that although *U. batuffolosa* is likely to suffer from long-term and excessive high solar irradiance and high seawater temperatures that will reduce its photosynthetic efficiency and eventually damage its photosynthetic apparatus, this species is still well adapted to support and tolerate the range of irradiance and temperature that characterized shallow tropical lagoon. Thus, it seems that photosynthesis is not an impediment to blooms by this species, which may explain the occurrence of green tides both during the warm and the cold seasons.

Acknowledgments

This project was funded by Direction du développement durable des territoires, Province Sud, New Caledonia, grant number C.458-19, ELADE project. The South Province of New Caledonia delivered the sampling authorizations (N°4406-2018/ARR/DENV).

We would like to thank Miguel Clarke, Benoit Soulard and Alan Choupeau for their logistical support during field campaigns. We also thanks Laurent Millet, Clarisse Majorel, and Claire Bonneville from the “Plateforme du vivant”, where genetic analyses were performed to support algae identification.

CRediT author statement

TJ: conceptualization, methodology, formal analysis, investigation, data curation, writing - reviewing & editing; **MB:** conceptualization, methodology, software, formal analysis, investigation, data curation, writing - reviewing & editing; **LL:** methodology, formal analysis, writing - reviewing & editing; **CP:** conceptualization, writing - reviewing & editing, project administration, funding acquisition; **SG:** formal analysis, investigation; **RL:** methodology, software, formal analysis, investigation, data curation, writing - reviewing & editing; **SVW:** conceptualization, methodology, software, formal analysis, investigation, data curation, writing - reviewing & editing; project administration, funding acquisition

References

Andrefouet, S., Cabioch, G., Flamand, B., Pelletier, B., 2009. A reappraisal of the diversity of geomorphological and genetic processes of New Caledonian coral reefs: a synthesis from optical remote sensing, coring and acoustic multibeam observations. Coral Reefs 28, 691-707.

Beer, S., Björk M., Gademan, R., Ralph, P., 2001. Measurements of photosynthesis in seagrass. In: Short FT, Coles R (eds) Global seagrass research methods. Elsevier, Amsterdam, pp 183–198

Beer, S., Björk, M., Beardall, J., 2014. Photosynthesis in the marine environment. John Wiley & Sons.

Berges, J.A., Charlebois, D.O., Mauzerall, D.C., Falkowski, P.G., 1996. Differential effects of nitrogen limitation on photosynthetic efficiency of photosystems I and II in microalgae. Plant Physiol. 110, 689-696.

Bischof, K., Rautenberger, R., Brey, L., Perez-Llorens, J.L., 2006. Physiological acclimation to gradients of solar irradiance within mats of the filamentous green macroalga *Chaetomorpha linum* from southern Spain. Mar. Ecol. Prog. Ser. 306, 165-175.

Brisset, M., Van Wynsberge, S., Andréfouët, S., Payri, C., Soulard, B., Bourassin, E., Gendre, R.L., Coutures, E., 2021. Hindcast and near real-time monitoring of green macroalgae blooms in shallow coral reef lagoons using sentinel-2: A New-Caledonia case study. Remote Sensing 13, 211.

Campbell, D.A., Tyystjarvi, E., 2012. Parameterization of photosystem II photoinactivation and repair. Biochim. Biophys. Acta 1817, 258-265.

Campbell, S.J., McKenzie, L.J., Kerville, S.P., 2006. Photosynthetic responses of seven tropical seagrasses to elevated seawater temperature. J. Exp. Mar. Biol. Ecol. 330, 455-468.

Carr, H., Bjork, M., 2007. Parallel changes in non-photochemical quenching properties, photosynthesis and D1 levels at sudden, prolonged irradiance exposures in *Ulva fasciata* Delile. J. Photochem. Photobiol. 87, 18-26.

Chin, T.M., Vazquez-Cuervo, J., Armstrong, E.M., 2017. A multi-scale high-resolution analysis of global sea surface temperature. Remote Sens. Environ. 200, 154-169.

Cleveland, J.S., Perry, M.J., 1987. Quantum yield, relative specific absorption and fluorescence in nitrogen limited *Chaetoceros gracilis*. Mar. Biol. 94, 489-497.

406 Conan, P., Joux, F., Torreton, J.P., Pujo-Pay, M., Douki, T., Rochelle-Newall, E., Mari, X., 2008.
407 Effect of solar ultraviolet radiation on bacterio- and phytoplankton activity in a large coral reef
408 lagoon (southwest New Caledonia). Aquat. Microb. Ecol. 52, 83-98.
409 Consalvey, M., Perkins, R.G., Paterson, D.M., Underwood, G.J.C., 2005. Pam fluorescence: A
410 beginners guide for benthic diatomists. Diatom Res. 20, 1-22.
411 Cosgrove, J., Borowitzka, M.A., 2010. Chlorophyll Fluorescence Terminology: An Introduction, in:
412 Suggett, D.J., Prášil, O., Borowitzka, M.A. (Eds.), Chlorophyll a Fluorescence in Aquatic
413 Sciences: Methods and Applications. Springer Netherlands, Dordrecht, pp. 1-17.
414 Coulombier, N., Blanchier, P., Le Dean, L., Barthelemy, V., Lebouvier, N., Jauffrais, T., 2021. The
415 effects of CO2-induced acidification on *Tetraselmis* biomass production, photophysiology and
416 antioxidant activity: a comparison using batch and continuous culture. J. Biotech. 325, 312-324.
417 Courtial, L., Roberty, S., Shick, J.M., Houlbrèque, F., Ferrier-Pagès, C., 2017. Interactive effects of
418 ultraviolet radiation and thermal stress on two reef-building corals. Limnol. Oceanogr. 62, 1000-
419 1013.
420 Cui, J.J., Zhang, J.H., Huo, Y.Z., Zhou, L.J., Wu, Q., Chen, L.P., Yu, K.F., He, P.M., 2015.
421 Adaptability of free-floating green tide algae in the Yellow Sea to variable temperature and light
422 intensity. Mar. Pollut. Bull. 101, 660–666
423 Enríquez, S., Borowitzka, M.A., 2010. The use of the fluorescence signal in studies of seagrasses and
424 macroalgae, in: Suggett, D.J., Prášil, O., Borowitzka, M.A. (Eds.), Chlorophyll a fluorescence in
425 aquatic sciences: Methods and applications. Springer Netherlands, Dordrecht, pp. 187-208.
426 Falkowski, P.G., Laroche, J., 1991. Acclimation to spectral irradiance in algae. J. Phycol. 27, 8-14.
427 Figueroa, F.L., Israel, A., Neori, A., Martinez, B., Malta, E.J., Ang, P., Inken, S., Marquardt, R.,
428 Korbee, N., 2009. Effects of nutrient supply on photosynthesis and pigmentation in *Ulva*
429 *lactuca* (Chlorophyta): responses to short-term stress. Aquat. Biol. 7, 173-183.
430 Figueroa, F.L., Salles, S., Aguilera, J., Jimenez, C., Mercado, J., Vinegla, B., FloresMoya, A.,
431 Altamirano, M., 1997. Effects of solar radiation on photoinhibition and pigmentation in the red
432 alga *Porphyra leucosticta*. Mar. Ecol. Prog. Ser. 151, 81-90.

Franklin, L.A., 1994. The effects of temperature-acclimation on the photoinhibitory responses of *Ulva-rotundata* blid. Planta 192, 324-331.

Franklin, L.A., Forster, R.M., 1997. The changing irradiance environment: consequences for marine macrophyte physiology, productivity and ecology. Eur. J. Phycol. 32, 207-232.

Franklin, L.A., Levavasseur, G., Osmond, C.B., Henley, W.J., Ramus, J., 1992. 2 components of onset and recovery during photoinhibition of *Ulva-rotundata*. Planta 186, 399-408.

Geider, R.J., Laroche, J., Greene, R.M., Olaizola, M., 1993. Response of the photosynthetic apparatus of *Phaeodactylum tricornutum* (Bacillariophyceae) to nitrate, phosphate, or iron starvation. J. Phycol. 29, 755-766.

Goss, R., Jakob, T., 2010. Regulation and function of xanthophyll cycle-dependent photoprotection in algae. Photosynthesis Res. 106, 103-122.

Henley, W.J., Ramus, J., 1989. Time course of physiological-response of *Ulva-rotundata* to growth irradiance transitions. Mar. Ecol. Prog. Ser. 54, 171-177.

Hersbach, H., Bell, B., Berrisford, P., Hirahara, S., Horányi, A., Muñoz-Sabater, J., Nicolas, J., Peubey, C., Radu, R., Schepers, D., Simmons, A., Soci, C., Abdalla, S., Abellan, X., Balsamo, G., Bechtold, P., Biavati, G., Bidlot, J., Bonavita, M., De Chiara, G., Dahlgren, P., Dee, D., Diamantakis, M., Dragani, R., Flemming, J., Forbes, R., Fuentes, M., Geer, A., Haimberger, L., Healy, S., Hogan, R.J., Hólm, E., Janisková, M., Keeley, S., Laloyaux, P., Lopez, P., Lupu, C., Radnoti, G., de Rosnay, P., Rozum, I., Vamborg, F., Villaume, S., Thépaut, J.-N., 2020. The ERA5 global reanalysis. Quarterly Journal of the Royal Meteorological Society 146, 1999-2049.

Horimoto, R., Masakiyo, Y., Ichihara, K., 2011. Enteromorpha-like *Ulva* (Ulvophyceae, Chlorophyta) growing in the Todoroki river, Ishigaki island, Japan, with special reference to *Ulva meridionalis* Horimoto et Shimada, sp. nov.. Bull. Natl. Museum Nat. Sci. Ser. B, Bot. 37, 155–167.

Huot, Y., Babin, M., 2010. Overview of fluorescence protocols: Theory, basic concepts, and practice, in: Suggett, D.J., Prášil, O., Borowitzka, M.A. (Eds.), Chlorophyll a fluorescence in aquatic sciences: Methods and applications. Springer Netherlands, Dordrecht, pp. 31-74.

Huo, Y., Kim, J.K., Yarish, C., Augyte, S., He, P., 2021. Responses of the germination and growth of Ulva prolifera parthenogametes, the causative species of green tides, to gradients of temperature and light. Aquat. Bot. 170, 103343.

Jauffrais, T., Jesus, B., Méléder, V., Turpin, V., Russo, A.D.A.P.G., Raimbault, P., Martin-Jézéquel, V., 2016. Physiological and photophysiological responses of the benthic diatom *Entomoneis paludosa* (Bacillariophyceae) to dissolved inorganic and organic nitrogen in culture. Mar. Biol. 163, 1-14.

Kirk, J.T.O., 1994. Light and Photosynthesis in Aquatic Ecosystems, 2 ed. Cambridge University Press, Cambridge.

Kraft, L.G.K., Kraft, G.T., Waller, R.F., 2010. Investigations into southern Australian *Ulva* (Ulvophyceae, Chlorophyta) taxonomy and molecular phylogeny indicate both cosmopolitanism and endemic cryptic species. J. Phycol. 46, 1257–1277.

Krause, G.H., Weis, E., 1991. Chlorophyll fluorescence and photosynthesis - the basics. Annu. Rev. Plant. Physiol. Plant. Mol. Biol. 42, 313-349.

Krupnik, N., Rinkevich, B., Paz, G., Douek, J., Lewinsohn, E., Israel, A., Carmel, N., Mineur, F., Maggs, C.A., 2018. Native, invasive and cryptogenic *Ulva* species from the Israeli Mediterranean Sea: Risk and potential. Mediterr. Mar. Sci. 19, 132–146.

Lagourgue, L., Gobin, S., Brisset, M., Vanderberghe, S., Bonneville, C., Jauffrais, T., Van Wynsberge, S., Payri, C.E., 2022. Ten new species of *Ulva* (Ulvophyceae, Chlorophyta) discovered in New Caledonia: Genetic and morphological diversity, and bloom potential. Eur. J. Phycol. 1-21. In press. https://doi.org/10.1080/09670262.2022.2027023

Lapointe, B.E., 1981. The effects of light and nitrogen on growth, pigment content, and biochemical-composition of *Gracilaria-foliifera* v *Angustissima* (gigartinales, rhodophyta). J. Phycol. 17, 90-95.

Liu, D.Y., Keesing, J.K., Xing, Q.U., Shi, P., 2009. World's largest macroalgal bloom caused by expansion of seaweed aquaculture in China. Mar. Pollut. Bull. 58, 888-895.

Maxwell, K., Johnson, G.N., 2000. Chlorophyll fluorescence - a practical guide. J. Exp. Bot. 51, 659-668.

Masakiyo, Y., Shimada, S., 2014. Species Diversity of the genus Ulva (Ulvophyceae, Chlorophyta) in Japanese waters, with special reference to *Ulva tepida* Masakiyo et S. Shimada sp. Nov.. Bull. Natl. Museum Nat. Sci. Ser. B, Bot. 40, 1–13.

Melton, J.T., Lopez-Bautista, J.M., 2020. Diversity of the green macroalgal genus *Ulva* (Ulvophyceae, Chlorophyta) from the east and gulf coast of the United States based on molecular data. J. Phycol. 57, 551-568

Platt, T., Gallegos, C.L., Harrison, W.G., 1980. Photoinhibition of photosynthesis in natural assemblages of marine phytoplancton J. Mar. Res. 38, 687-701.

Pringault, O., de Wit, R., Camoin, G., 2005. Irradiance regulation of photosynthesis and respiration in modern marine microbialites built by benthic cyanobacteria in a tropical lagoon (New Caledonia). Microb. Ecol. 49, 604-616.

Ralph, P.J., Gademann, R., 2005. Rapid light curves: A powerful tool to assess photosynthetic activity. Aquat. Bot. 82, 222-237.

Ralph, P.J., Gademann, R., Larkum, A.W.D., Kuhl, M., 2002. Spatial heterogeneity in active chlorophyll fluorescence and PSII activity of coral tissues. Mar. Biol. 141, 639-646.

Raven, J.A., Geider, R.J., 2003. Adaptation, acclimation and regulation in algal photosynthesis, in: Larkum, A.W.D., Douglas, S.E., Raven, J.A. (Eds.), Photosynthesis in Algae. Springer Netherlands, Dordrecht, pp. 385-412.

Richardson, K., Beardall, J., Raven, J.A., 1983. Adaptation of unicellular algae to irradiance - an analysis of strategies. New Phytologist 93, 157-191.

Scherner, F., Barufi, J.B., Horta, P.A., 2012. Photosynthetic response of two seaweed species along an urban pollution gradient: Evidence of selection of pollution-tolerant species. Mar. Pollut. Bull. 64, 2380-2390.

Schofield, O., Evens, T.J., Millie, D.F., 1998. Photosystem II quantum yields and Xanthophyll-cycle pigments of the macroalga *Sargassum natans* (Phaeophyceae): Responses under natural sunlight. J. Phycol. 34, 104-112.

513 Schreiber, U., Bilger, W., Neubauer, C., 1994. Chlorophyll fluorescence as a non-intrusive indicator
514 for rapid assessment of in vivo photosynthesis, in: Schulze, E., Caldwell, M.M. (Eds.),
515 Ecophysiology of Photosynthesis. Springer-Verlag, Berlin, pp. 49-70.
516 Thiers, B. 2019. Index herbariorum: a global directory of public herbaria and associated staff. New
517 York Botanical Garden's Virtual Herbarium.
518 Torregiani, J.H., Lesser, M.P., 2007. The effects of short-term exposures to ultraviolet radiation in the
519 Hawaiian Coral *Montipora verrucosa*. J. Exp. Mar. Biol. Ecol. 340, 194-203.
520 Uhrmacher, S., Hanelt, D., Nultsch, W., 1995. Zeaxanthin content and the degree of photoinhibition
521 are linearly correlated in the brown alga *Dictyota-dichotoma*. Mar. Biol. 123, 159-165.
522 Wang, Y., Qu, T., Zhao, X., Tang, X., Xiao, H., Tang, X., 2016. A comparative study of the
523 photosynthetic capacity in two green tide macroalgae using chlorophyll fluorescence.
524 SpringerPlus 5, 775. https://doi.org/10.1186/s40064-016-2488-7
525 Whitehouse, L.N.A., Lapointe, B.E., 2015. Comparative ecophysiology of bloom-forming macroalgae
526 in the Indian River Lagoon, Florida: *Ulva lactuca, Hypnea musciformis,* and *Gracilaria*
527 *tikvahiae*. J. Exp. Mar. Biol. Ecol. 471, 208-216.
528 Williamson, C.J., Perkins, R., Yallop, M.L., Peteiro, C., Sanchez, N., Gunnarsson, K., Gamble, M.,
529 Brodie, J., 2018. Photoacclimation and photoregulation strategies of *Corallina* (Corallinales,
530 Rhodophyta) across the NE Atlantic. Eur. J. Phycol. 53, 290-306.
531 Xie, W.F., Wu, C.H., Zhao, J., Lin, X.Y., Jiang, P., 2020. New records of *Ulva* spp. (Ulvophyceae,
532 Chlorophyta) in China, with special reference to an unusual morphology of *U. meridionalis*
533 forming green tides. Eur. J. Phycol. 55, 412–425.
534 Xu, Z., Wu, H., Zhan, D., Sun, F., Sun, J., Wang, G., 2014. Combined effects of light intensity and
535 NH_4^+-enrichment on growth, pigmentation, and photosynthetic performance of *Ulva prolifera*
536 (Chlorophyta). Chinese J. Oceanol. Limnol. 32, 1016-1023.
537 Zhang, X.W., Mou, S.L., Cao, S.N., Fan, X., Xu, D., Ye, N.H., 2015. Roles of the transthylakoid
538 proton gradient and xanthophyll cycle in the non-photochemical quenching of the green alga
539 *Ulva linza*. Estuar. Coast. Shelf Sci. 163, 69-74
540

Tables

Table 1. Fluorescence parameters, definition, implementation and derivation (adapted from Cosgrove and Borowitzka, 2010; Williamson et al., 2018)

Parameter	definition	Condition	Derivation
F'	The initial fluorescence intensity	Light incubated	
Fm'	The maximum intensity under saturating light	Light incubated	
Fm'm	The maximum value of Fm'	Light incubated	
Fq'	The fluorescence quenched in actinic light	Light incubated	$\mathrm{Fm'} - \mathrm{F'}$
Fq'/Fm'	Effective quantum efficiency of PSII	Light incubated	
F0	The minimum fluorescence yield (all RCIIs are open, dark-regulated)	Dark incubated	
Fm	The maximum fluorescence under saturating light (all RCIIs are open with NPQ negligible, dark-regulated)	Dark incubated	
Fv	The maximal variable fluorescence (dark-regulated)	Dark incubated	$\mathrm{Fm} - \mathrm{F0}$
Fv/Fm	Maximum quantum efficiency of PSII (dark-regulated)	Dark incubated	$\frac{\mathrm{Fm} - \mathrm{F0}}{\mathrm{Fm}}$
NPQ	Non photochemical quenching	Dark incubated	$\frac{\mathrm{Fm} - \mathrm{Fm'}}{\mathrm{Fm'}}$
PAR	Photosynthetically active radiation (µmol photons m^{-2} s^{-1})	Light & dark incubated	
rETR	Relative Electron transport rate (through PSII)	Light & dark incubated	$F_q'/F_m' \times PAR \times 0.5$
rETR(I)	Relative Electron transport rate (through PSII) as function of the irradiance and estimated by adjusting the model by Platt et al. (1980) to the rapid light curve data	Light & dark incubated	$rETR_m \times \left(1 - \mathrm{e}^{\left(-\alpha \times \frac{\mathrm{I}}{rETR_m}\right)}\right) \times \mathrm{e}^{\left(-\beta \times \frac{\mathrm{I}}{rETR_m}\right)}$
rETRmax	The maximum relative electron transport rate	Light & dark incubated	$rETR_m \times \left(\frac{\alpha}{\alpha+\beta}\right) \times \left(\frac{\beta}{\alpha+\beta}\right)^{\frac{\beta}{\alpha}}$
alpha (α)	The initial slope of the RLC at limiting irradiance	Light & dark incubated	
beta (β)	The slope when photoinhibition occurred	Light & dark incubated	
Ek	The light saturation index (µmol photons m−2 s−1)	Light & dark incubated	$\frac{rETR_{max}}{\alpha}$

546 **Table 2**. Results of the statistical analysis testing differences in photosynthetic parameters of *Ulva*
547 *batuffolosa* between the five field campaigns. Photosynthetic parameters were obtained from rapid
548 light curves performed light and dark incubated conditions. Statistical tests used were either ANOVAs
549 or Kruskal-wallis tests (*). Fq'/Fm' and Fv/Fm stand for Effective and Maximum quantum light
550 utilization efficiency of Photosystem II (PSII); $rETR_{max}$, maximum relative electron transport rate in
551 AU; Ek, light saturation coefficient in μmol photons m^{-2} s^{-1}; alpha, maximum light utilization
552 coefficient for PS II; beta, photoinhibition coefficient for PSII. Significant p-values (< 0.05) are
553 bolded.

	Light incubated		Dark incubated	
	F-Ratio	P-Value	F-Ratio	P-Value
Fq'/Fm', Fv/Fm	2.60	0.100	3.70	**0.042**
$rETR_{max}$	8.32	**0.003**	13.32	**0.001**
Ek	15.48	**<0.001**	4.49	**0.025**
alpha	3.88	**0.037**	4.38	**0.027**
beta*		**0.034**		0.406

554

555

Table 3. Results of the general linear model analysis on Non-Photochemical Quenching (NPQ) of *Ulva batuffolosa* between the different field campaigns (month) and over the induction and dark recovery (light/dark condition). Significant p-values (< 0.05) are bolded.

	NPQ	
	F-Ratio	P-Value
A: Field campaign	86.20	**<0.001**
B: Light/dark condition	49.53	**<0.001**
A:B	1.83	**0.012**

562 **Figure legends**

563

564 **Fig. 1.** Study site. **A**. Location of the Poé-Gouaro-Deva (PGD) lagoon in New Caledonia. **B**. Satellite
565 view of the PGD lagoon, highlighting the location of B21 station. The picture shows/points an
566 underwater view of the green algal during a bloom of *Ulva batuffolosa* at this station.

567

568 **Fig. 2.** Environmental conditions that characterized the PGD area over the study period. **A.**
569 Temperature, at B21 station, as recorded by loggers (solid line) or satellite derived SST (grey dashed
570 line). Grey ribbon delimits the daily minimum and maximum temperature recorded by *in situ* loggers.
571 **B**. Surface Solar Radiation Downwards (SSRD). Note that night values were not discarded to compute
572 this time series, but were discarded to compute values reported in the main text. Dashed red lines mark
573 the five sampling campaigns, respectively on the 16th May 2019, 09th July 2019, 18th November 2019,
574 19th February 2020, and 25th May 2020.

575

576 **Fig 3.** Algal biomass (g Dry Weight m^{-2}) recorded during field campaigns along transects with
577 corresponding under water images for illustration. Letters indicate significant differences between
578 campaigns (p-value < 0.05). Data are expressed as mean ± standard deviation (SD, n = 3).

579

580 **Fig. 4. A.** Effective (Fq'/Fm') and **B.** Maximum quantum light utilization efficiency of the
581 photosystem II (PSII, Fv/Fm) measured under ligh and dark incubated conditions, respectively, for
582 *Ulva batuffolosa* collected in the PGD lagoon during the five field campaigns. Data are expressed as
583 mean ± standard error (SE, n = 3) and * indicates significant differences between field campaigns (p-
584 value < 0.05).

585

586 **Fig. 5. A.** Light and **B.** Dark incubated rapid light curves (RLC, n=3) expressed as the relative electron
587 transport rate (rETR) as a function of the photosynthetic active radiation (PAR in µmol photons m^{-2} s^{-1}) of *Ulva batuffolosa* in PGD lagoon over one year. Data are expressed as mean ± standard deviation
589 (SD, n = 3).
590

591 **Fig. 6**. Photosynthetic parameters obtained from rapid light curves carried out on light (yellow) and
592 dark (grey) incubated *Ulva batuffolosa* during the different field campaigns. **A.** Maximum electron
593 transport rate, $rETR_{max}$ in AU, **B.** light saturation coefficient, Ek in µmol photons m^{-2} s^{-1}, **C.** Maximum
594 light utilization coefficient for photosystem II, alpha, **D.** photoinhibition coefficient for photosystem
595 II, beta. Data are expressed as mean ± standard error (SE, n = 3) and different letters indicate
596 statistically significant differences ($p < 0.05$).
597

598 **Fig. 7.** Non-Photochemical Quenching (NPQ) over the induction (yellow background) and dark
599 recovery (grey background) of *Ulva batuffolosa* sampled at the different period of the year and dark
600 incubated. Data are expressed as mean ± standard deviation (SD, n = 3) and different letters (cf.
601 caption) indicate statistically significant differences between field campaigns ($p < 0.05$).

Figures

Fig. 1

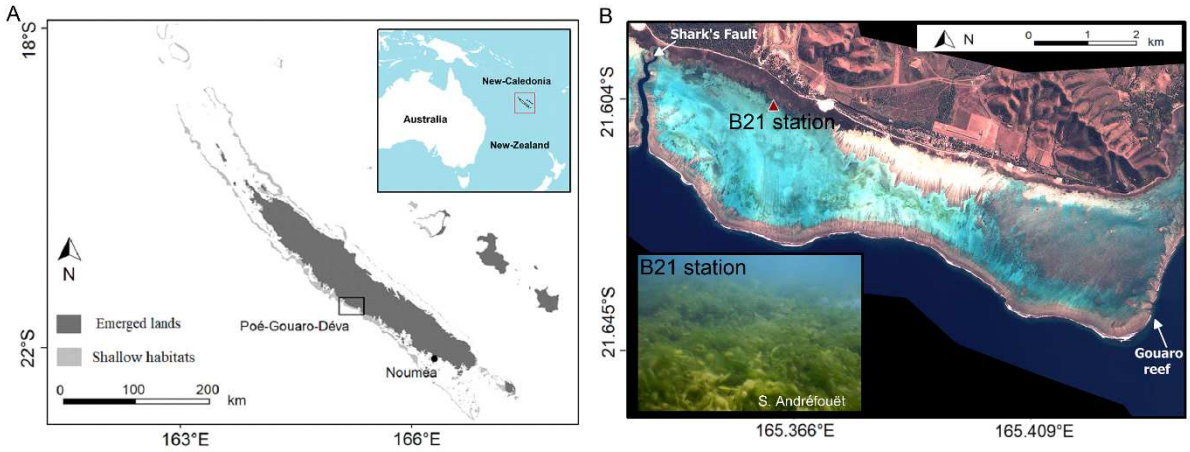

Fig. 2

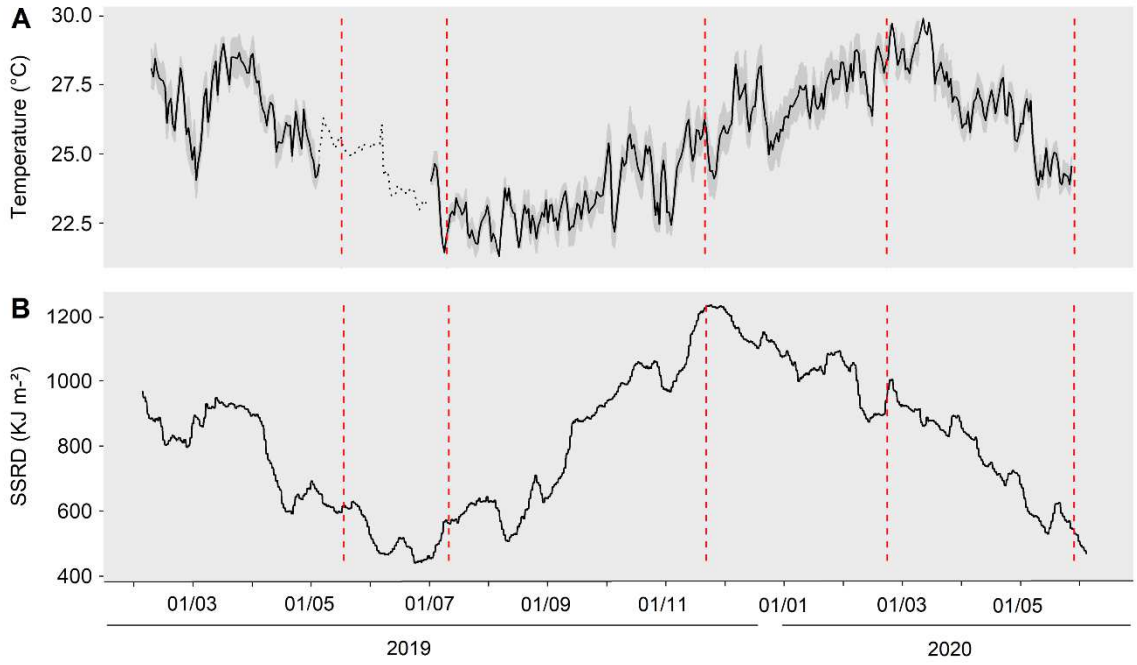
A
30.0
27.5
25.0
22.5
Temperature (°C)
B
1200
1000
800
600
400
SSRD (KJ m-2)
01/03
01/05
01/07
01/09
01/11
01/01
01/03
01/05
2019
2020

Fig. 3

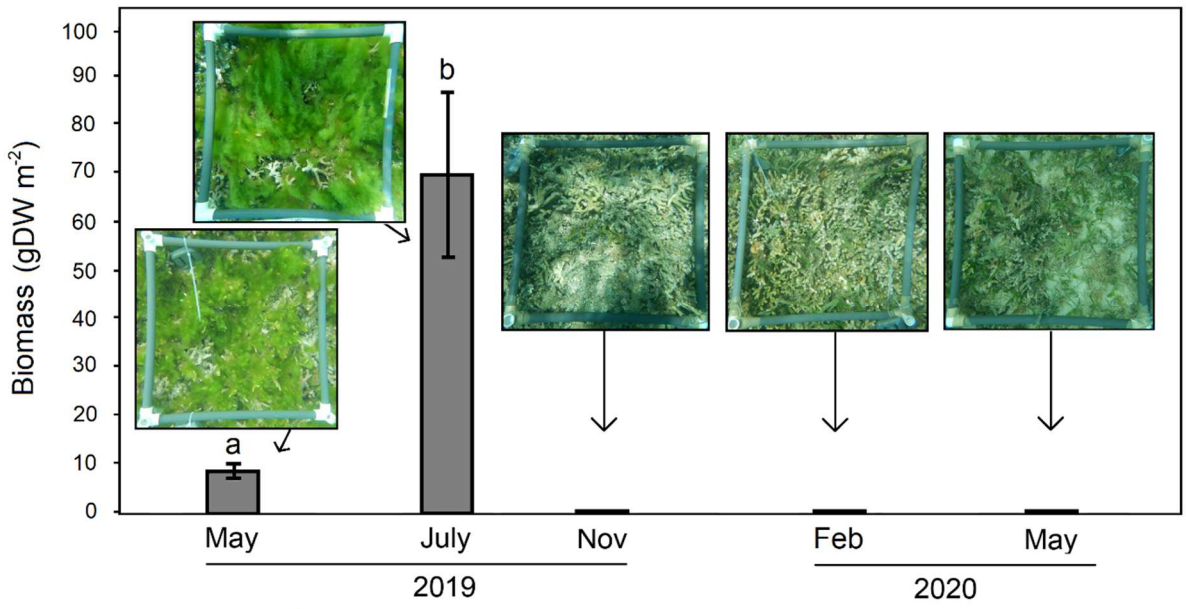
Biomass (gDW m-2)
100
90
80
70
60
50
40
30
20
10
0
a
b
May
July
Nov
Feb
May
2019
2020

Fig. 4

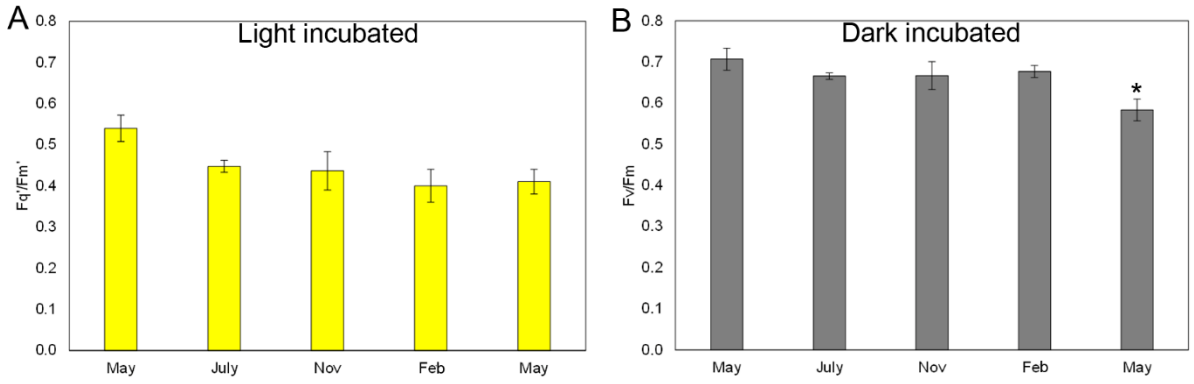
A
Light incubated
Fq'/Fm'
0.8
0.7
0.6
0.5
0.4
0.3
0.2
0.1
0.0
May
July
Nov
Feb
May
B
Dark incubated
Fv/Fm
*
May
July
Nov
Feb
May

Fig. 5

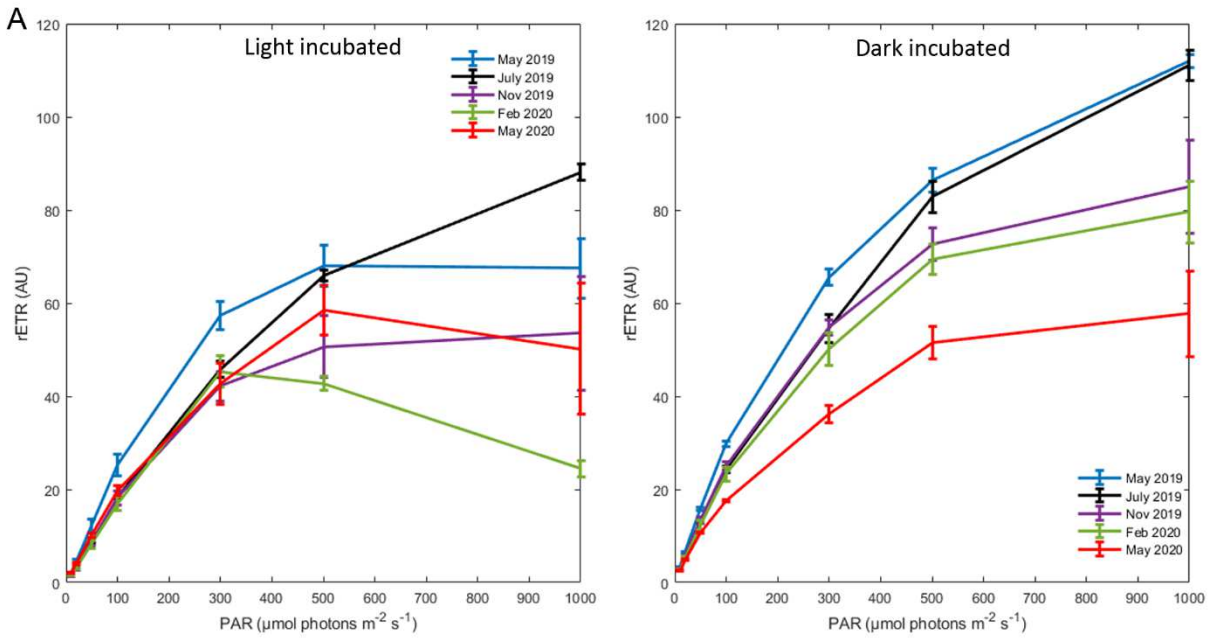
A
Light incubated
Dark incubated
May 2019
July 2019
Nov 2019
Feb 2020
May 2020
rETR (AU)
PAR (µmol photons m-2 s-1)
0
20
40
60
80
100
120
0
100
200
300
400
500
600
700
800
900
1000

Fig. 6

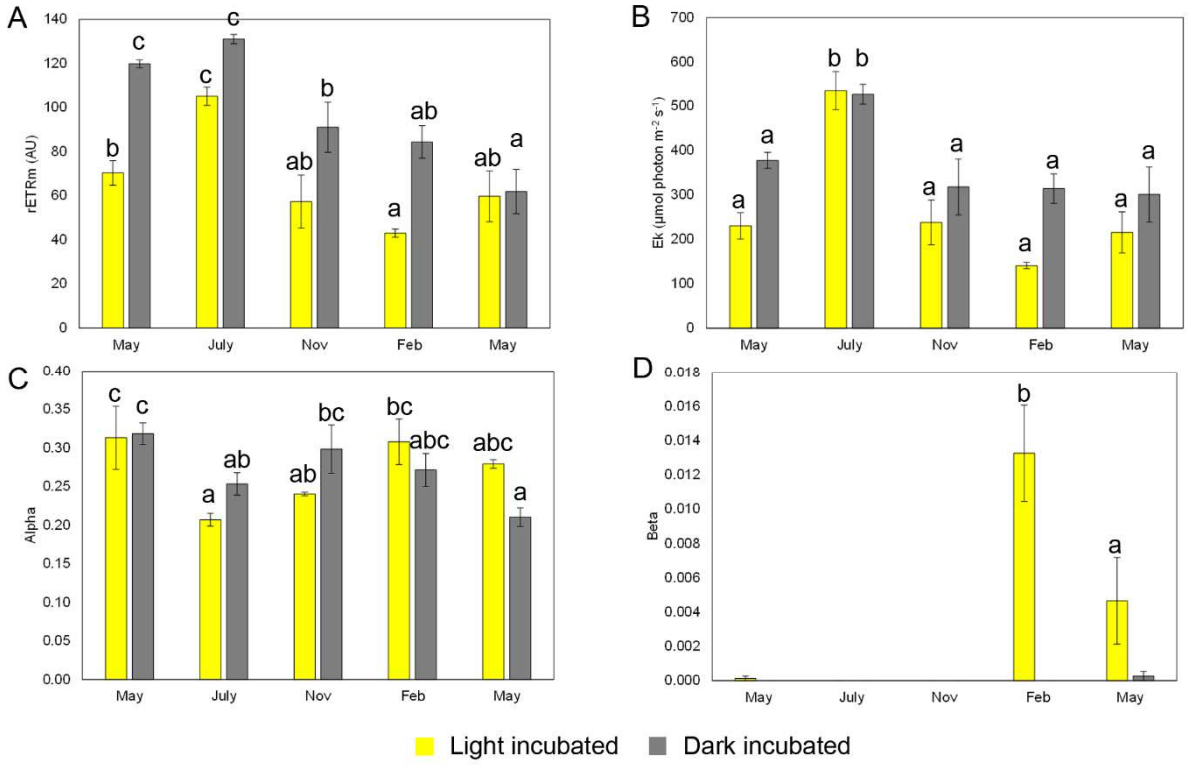
A
rETRm (AU)
140
120
100
80
60
40
20
0
b
c
c
c
ab
b
a
ab
ab
a
May
July
Nov
Feb
May
B
Ek (µmol photon m⁻² s⁻¹)
700
600
500
400
300
200
100
0
a
a
b b
a
a
a
a
a
a
May
July
Nov
Feb
May
C
Alpha
0.40
0.35
0.30
0.25
0.20
0.15
0.10
0.05
0.00
c
c
a
ab
ab
bc
bc
abc
abc
a
May
July
Nov
Feb
May
D
Beta
0.018
0.016
0.014
0.012
0.010
0.008
0.006
0.004
0.002
0.000
b
a
May
July
Nov
Feb
May
Light incubated
Dark incubated

Fig. 7

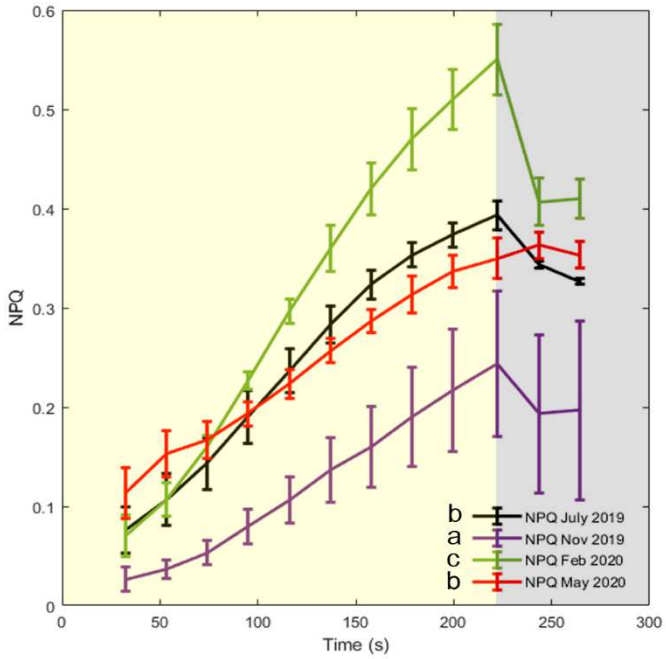
NPQ
Time (s)
0
0.1
0.2
0.3
0.4
0.5
0.6
0
50
100
150
200
250
300
b
a
c
b
NPQ July 2019
NPQ Nov 2019
NPQ Feb 2020
NPQ May 2020